# A Data-driven approach to Determining the Fidelity in the Hardware-in-the-loop Systems using Subspace Identification Method

February 2024

Sai Pushpak Nandanoori
Kristine Arthur-Durett
Alejandro Heredia-Langner
Thomas Edgar

**DISCLAIMER**

This report was prepared as an account of work sponsored by an agency of the United States Government. Neither the United States Government nor any agency thereof, nor Battelle Memorial Institute, nor any of their employees, makes **any warranty, express or implied, or assumes any legal liability or responsibility for the accuracy, completeness, or usefulness of any information, apparatus, product, or process disclosed, or represents that its use would not infringe privately owned rights**. Reference herein to any specific commercial product, process, or service by trade name, trademark, manufacturer, or otherwise does not necessarily constitute or imply its endorsement, recommendation, or favoring by the United States Government or any agency thereof, or Battelle Memorial Institute. The views and opinions of authors expressed herein do not necessarily state or reflect those of the United States Government or any agency thereof.

# A Data-driven approach to Determining the Fidelity in the Hardware-in-the-loop Systems using Subspace Identification Method

February 2024

Sai Pushpak Nandanoori
Kristine Arthur-Durett
Alejandro Heredia-Langner
Thomas Edgar

# Abstract

One of the major questions in any Hardware-in-the loop (HiL) simulation is to understand the fidelity of the HiL simulation itself which is most often indicated qualitatively as either high or low instead of quantifying it. Being cognizant of the level of fidelity forms the crux to assess the validity and credibility of the HiL simulation. In this work, we address this issue by developing a systematic, data-driven approach to assess the fidelity of any HiL simulation, and more specifically, the fidelity of the interface between the simulator and hardware in an HiL simulation. Applying a subspace identification method, a linear system representing the interface is obtained from the time-series data captured between the hardware and simulator in the HiL simulation. Finally, the fidelity is defined based on this linear system properties. The proposed data-driven fidelity quantification framework is illustrated on the IEEE 123 node feeder system running on HYPERSIM and interacting with virtual protection relays.

# Acknowledgment

# Contents

# Figures

# 1.0 Introduction

The possibility of service interruptions or other unforeseen issues discourages the demonstration of novel control approaches on actual systems. Therefore, suggested control strategies and other design changes are tested using simulation models before being applied to the real system, especially in difficult circumstances. Hardware-in-the-loop (HiL) simulation is a simulation type that includes hardware components along with a simulator connected via an interface. This approach has many advantages as a number of low probability extreme test cases can be simulated with minimal effort and expenditure. However, there is a trade-off between the cost and fidelity of the HiL simulation, which indicates how close the HiL simulation is when compared to the real world case.

There are numerous interpretations of fidelity and to obtain a consistent definition, we recall the formal definition for fidelity briefly as defined by the simulation interoperability standards organization fidelity implementation study group (FISG) [1], [2] *The degree to which a model or simulation reproduces the state and behavior of a real world objector the perception of a real world object, feature, condition, or chosen standard in a measurable or perceivable manner.*

The FISG report is referred to by the Department of Defense Modeling and Simulation Enterprise [3] where they explain fidelity as the accuracy of the representation when compared to the real world. Fidelity is thus characterized as the faithfulness of the simulation and in general may be described with respect to measures, standards or perceptions that include: Accuracy, Precision, Repeatability, Resolution, Scope, Sensitivity [1], [4].
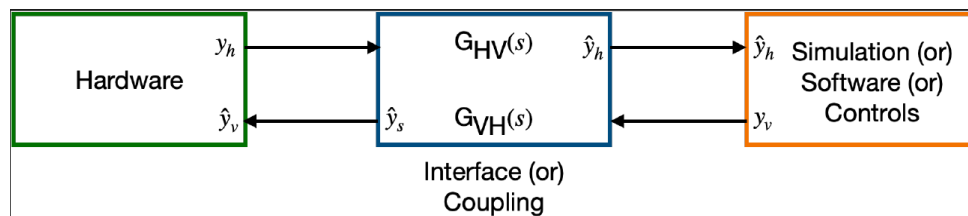


Figure 1: HiL Setup: The simulations and the hardware interacting with each other via the interface (or) coupling.

This work aims to understand the fidelity of hardware-in-the- loop (HiL) simulation setups. Depending on the scope of the HiL simulation, fidelity could be studied in two different settings. (a) Fidelity of the HiL setup when compared to a real system and (b) fidelity of the interface (see Fig. 1 for a representation of interface in the HiL simulation set up) in a HiL simulation. In the scope of this work, we focus on studying the fidelity of the interface in the HiL simulation. The motivation of this work is to understand the question of whether the interface in an HiL simulation can communicate data between the simulator and the hardware perfectly, without any delay, attenuation, amplification, or data loss. In addition, can we measure the fidelity of the interface in a quantitative way, as opposed to making a qualitative judgment of whether it is high or low? This is a difficult question to answer, as it depends on the specific HiL simulation setup and the use case. The scope of this work focuses on developing metrics to characterize the fidelity of the interface in the HiL simulations such that we can assert, *'The interface of the HiL simulation provides X amount of fidelity for a Y use case'.*

## 1.1   Related Work and State-of-the-Art

The authors of the work, [5] generally define the notion of fidelity, verifiability and validity for a simulation, however, nothing in particular to the HiL simulations. Aside from the work by the simulation interoperability standards organization FISG [1], [4], one of the initial works to discuss the HiL simulation fidelity framework is the work by Roza [6] in 2001, where an unified fidelity framework is developed that provides a fundamental methodology to simulation fidelity assessment process. Another work that focus on accuracy of HiL simulation is [7], however, the authors in this work don't assume access to the real system output and identify an upper bound to the accuracy of the HiL simulation. Their accuracy is computed in the frequency domain based on the transfer function of the simulator, hardware and the transfer function of the interface. The authors in [8] focus on the accuracy of HiL simulations and to quantify they assume having access to the simulation output as well the real system output. The accuracy is then calculated as a difference of those datasets. In [9], Typhoon HiL, Inc study the fidelity of the controller HiL (CHiL) simulation by visually comparing the output current of the CHiL system and the real systemin several test-cases. The work [10] defines transparency todefine the fidelity of the HiL simulation. The idea behind the definition of transparency is to ensure the data communicated by the simulator is received as it is by the hardware and vice versa. This work assumes having access to the model of the interface and computes the transparency and thereby fidelity in the frequency domain.

A recent study laying out the requirements for a Power HiL (PHiL) simulation is [11]. The authors of this work use accuracy as a measure and outlines necessary requirements for the implementation of PHiL simulations. Most recently,the PhD thesis of Sangeeth [12] serves as a detailed literature survey on various methods to study fidelity. The author develops a distance metric to define fidelity based on theory of formal verification, game theory and control by assuming the knowledge of the models. They present a consistent approach to evaluate fidelity of simulation models along the product development chain with a particular focus on Airbus operation studies.

One of the common aspects in almost all the existing works is the assumption on having access to the mathematical models for the interface. In this work, we overcome this assumption and identify the models from the time-series data using the subspace identification method (SIM) and further carry on the fidelity quantification study.

## 1.2   Contributions

We take a similar approach as in [10] to study the fidelity of the interface in an HiL simulation. However, this work does not assume the knowledge of the coupling model and obtains a model for the interface using the SIM which results in a linear system. Only the input and output data to the interface is used to identify the linear model and the corresponding transfer function. The summary of contributions are as follows:

- An algorithm to identify the model for the interface using the SIM from the time-series measurements.

- Fidelity quantification of the interface in a HiL simulation based on the interface system properties.

In the following, we briefly recall the mathematical preliminaries and recall the steps involved in the SIM to obtain the system matrices for the interface model.

# 2.0 Subspace Identification Methods

We begin this section with the necessary mathematical background on orthogonal and oblique projections [13, Chapter 1] that are helpful to understand the subspace identification method (SIM).

## 2.1 Orthogonal and Oblique Projections

**Orthogonal Projections:** The projection of row space of a matrix, $A \in \mathbb{R}^{p \times d}$ onto the row space of the matrix, $B \in \mathbb{R}^{q \times d}$ is given by

$$A/B := A\, \Pi_B = AB^\top (BB^\top)^\dagger B$$

Where $(\cdot)^\dagger$ denotes the Moore-Penrose pseudo inverse of matrix $(\cdot)$, $\Pi_B$ denotes the projection operator that projects the row space of matrix $A$ on the row space of matrix $B$. One of the implicit assumptions for this projection is that the columns of the matrices $A$ and $B$ are the same (here, $d$. The geometric operation that projects the row space of the matrix $\boldsymbol{A}$ onto the orthogonal complement of the row space of the matrix $\boldsymbol{B}$ is given by

$$A/B^\perp := A\Pi_{B^\perp}$$

where $\Pi_{B^\perp} = I_d - \Pi_B$, $I_d$ is the identity matrix of $d$ columns.

**Oblique Projections:** The oblique projection of the row space of $A \in R^{p \times d}$ along the row space of $B \in R^{q \times d}$ on the row space of $C \in R^{r \times d}$ is defined as:

$$A/BC := (A/B^\perp)(C/B^\perp)^\dagger C$$

## 2.2 Algorithmic Steps to Identify System Matrices

Consider the following linear discrete-time linear dynamical system:

$$x_{k+1} = A_d x_k + B_d u_k$$

$$y_k = C_d x_k + D_d u_k$$

Equation 1

The objective is to identify the system matrices $A_d, B_d, C_d, D_d$ given the input $(u_0, u_1, \dots)$ and output $(y_0, y_1, \dots)$ time-series data. In the scope of this work, the system matrices in Equation 1 are identified applying subspace identification methods.

In the following, we summarize the steps (from [13]) involved in identifying the state space system matrices for the self containment of this work. We refer the readers to [13] for rigorous technical treatment on this topic.

Let the input and output time-series data corresponding to a dynamical system be given by

$$U = \begin{bmatrix} u_0 & u_1 & \cdots & u_{i-1} & u_i & u_{i+1} & \cdots & u_{k-1} \end{bmatrix}$$
$$Y = \begin{bmatrix} y_0 & y_1 & \cdots & y_{i-1} & y_i & y_{i+1} & \cdots & y_{k-1} \end{bmatrix}$$

<p style="text-align:center">Equation 2</p>

where $u_j \in R^m, y_j \in R^{\mathbb{l}}$ for every $j \in \{0,1,2,\dots,k-1\}$. Note that a total of $k$ input and $k$ output measurements are considered here and $i$ is chosen in such a way that, $i < \frac{k}{2}$. The value of $i$ must at least be the maximum order of the system to be identified. To obtain the system state space matrices, Hankel matrices corresponding to the input and output time-series data are formed by choosing $j$ columns such that $j = k + 1 - 2i$. Furthermore, the input and output Hankelized time-series data is divided into two halves namely, *past* and *future* such that the measurements up to time $i + j - 2$ are treated as past and the measurements from time $i$ are considered future. Note that there is a overlap of $j - 1$ measurements in the past and future datasets manifested due to the time-delay embedding of the data formed via Hankel matrices.

The Hankelized input and output measurements corresponding to the `past' and `future' are denoted by $U\_p, U\_f$ and $Y\_p, Y\_f$ where the subscripts $p$ and $f$ indicating past and future. The $U\_p, U\_f$ matrices are given by

$$U_p = \begin{bmatrix} u_0 & u_1 & \cdots & u_{j-2} & u_{j-1} \\ u_1 & u_2 & \cdots & u_{j-1} & u_j \\ \vdots & \vdots & \ddots & \vdots & \vdots \\ u_{i-1} & u_i & \cdots & u_{i+j-3} & u_{i+j-2} \end{bmatrix}$$

$$U_f = \begin{bmatrix} u_i & u_{i+1} & \cdots & u_{i+j-2} & u_{i+j-1} \\ u_{i+1} & u_{i+2} & \cdots & u_{i+j-1} & u_{i+j} \\ \vdots & \vdots & \ddots & \vdots & \vdots \\ u_{2i-1} & u_{2i} & \cdots & u_{2i+j-3} & u_{2i+j-2} \end{bmatrix}$$

<p style="text-align:center">Equation 3</p>

where $U_p, U_f \in R^{mi}$. Another notation used in the literature [13], [14] to represent Hankel matrices, $U_p$ and $U_f$ considering the starting and ending time-point of the data is given by
$$U_{0|i-1} = U_p, \ U_{i|2i-1} = U_f$$
By appending the first row of $U_f$ as the last row of $U_p$, we obtain,
$$U_{0|i} = U_p^+, \ U_{i+1|2i-1} = U_f^-$$
where $U_p^+ \in R^{mi+m}$, $U_f^- \in R^{mi-m}$. Similarly, the past and future Hankel matrices, and their time-shifted matrices corresponding to output measurements are denoted by $Y_p, Y_f, Y_p^+, Y_f^-$ respectively. The matrices $Y_p, Y_f \in R^{\mathbb{l}i}$, $Y_p^+ \in R^{\mathbb{l}i+i}$ and $Y_f^- \in R^{\mathbb{l}i-\mathbb{l}}$. Finally, the combined input and output past Hankel matrix are defined as

$$W_p = \begin{bmatrix} U_p \\ Y_p \end{bmatrix}$$

where $W_p \in R^{mi+\mathbb{l}i}$. The matrices, $W_f, W_p^+, W_f^-$ are accordingly defined. With this, the algorithm to compute the system matrices $(A_d, B_d, C_d, D)$ is summarized as follows.

Subspace Identification Methods

---

**Algorithm 1** System Identification using the SIM [13]

1: **Input**: Input and output time-series measurements ($U$ and $Y$), choice of $i, j$ to obtain past and future datasets.

2: Form the past and future Hankel matrices:

$$U_p, Y_p, W_p, U_f, Y_f, W_f, U_p^+, Y_p^+, W_p^+, U_f^-, Y_f^-.$$

3: Obtain the oblique projections

$$\mathcal{O}_i = Y_f /_{U_f} W_p,$$
$$\mathcal{O}_{i-1} = Y_f^- /_{U_f^-} W_p^+.$$

4: Compute the SVD of the oblique projection as

$$O_i = \bar{\mathcal{U}} \bar{\mathcal{S}} \bar{\mathcal{V}}^\top.$$

5: Inspecting the singular values in $\bar{\mathcal{S}}$, determine the number of non-zero singular values which yields the order of the system being identified. Let the number of non-zero singular values be $n$. Then we have,

$$\bar{\mathcal{U}} = \begin{bmatrix} \mathcal{U} & * \end{bmatrix}, \bar{\mathcal{S}} = \begin{bmatrix} \mathcal{S} & 0 \\ 0 & 0 \end{bmatrix}, \bar{\mathcal{V}}^\top = \begin{bmatrix} \mathcal{V}^\top \\ * \end{bmatrix}.$$

Hence, we obtain, $\mathcal{O}_i \approx \mathcal{U}\mathcal{S}\mathcal{V}^\top$.

6: Determine the extended observability gramians corresponding to the underlying dynamical system, $\Gamma_i$ and $\Gamma_{i-1}$ as follows

$$\Gamma_i = \mathcal{U}\mathcal{S}^{1/2}.$$

$\Gamma_{i-1}$ is determined by removing the last $\ell$ (block) rows from $\Gamma_i$.

7: Determine the $i^{th}, i+1^{th}$ state values as shown below.

$$X_i = \Gamma_i^\dagger \mathcal{O}_i, \quad X_{i+1} = \Gamma_{i-1}^\dagger \mathcal{O}_{i-1}.$$

8: **Output**: Obtain the discrete-time linear system matrices corresponding to the underlying time-series data by solving the following least squares problem.

$$\min_{A_d, B_d, C_d, D_d} \left\| \begin{bmatrix} X_{i+1} \\ Y_{i|i} \end{bmatrix} - \begin{bmatrix} A_d & B_d \\ C_d & D_d \end{bmatrix} \begin{bmatrix} X_i \\ U_{i|i} \end{bmatrix} \right\|_F^2.$$

The solution to this optimization problem is obtained analytically as

$$\begin{bmatrix} A_d & B_d \\ C_d & D_d \end{bmatrix} = \begin{bmatrix} X_{i+1} \\ Y_{i|i} \end{bmatrix} \begin{bmatrix} X_i \\ U_{i|i} \end{bmatrix}^\dagger.$$

---

In the next section, we show how this linear system identification is applied to identify the transfer function of the interface (in a HiL simulation) and then compute its fidelity.

## 3.0 Fidelity Quantification

The main focus of this work is to understand whether the time-series measurements communicated between the software and the hardware via the interface reached as expected. We approach this problem by constructing the transfer function representing the interface and looking at the properties of the transfer function to understand how much the measurements have been modified by the interface. Based on this understanding a transparency measure is defined, such that, if the interface is (completely) transparent, then it has not modified the measurements communicated between the simulator and the hardware which results in complete fidelity in the HiL simulation. In the following, we discuss how to construct the transfer function corresponding to the interface from the time-series data of the HiL simulation following the SIM discussed in Section 2.0.

Let $y_v(t), y_h(t)$ denote the time-domain inputs to the interface from the simulation and the hardware respectively. Similarly, $\hat{y}_v(t), \widehat{y_h}(t)$ denote the time-domain outputs of the interface to the simulation and the hardware (see Figure 1). Let, $G_{HV}(s)$ be the transfer function of the interface with output, $\widehat{y_h}(t)$ and input $y_h(t)$. Similarly, $G_{VH}(s)$ denote the transfer function of the interface with output $\hat{y}_v(t)$ and input $y_v(t)$. We use $G_{VH}(s)$ to describe the main results of this work and the same results hold for $G_{HV}(s)$ as well.

*Assumption 1:* The interface is represented as a linear time invariant system.

*Remarks 2:* The assumption 1 is not restrictive as the interface is supposed to communicate the data between the simulation and the hardware without altering it. Hence, a linear model is sufficient to model the interface.

The input and output time-series data for the interface of a single input single output (SISO) interface is given by

$$Y_v^d = \begin{bmatrix} y_{v_0} & y_{v_1} & \cdots & y_{v_k} \end{bmatrix},$$
$$\hat{Y}_v^d = \begin{bmatrix} \hat{y}_{v_0} & \hat{y}_{v_1} & \cdots & \hat{y}_{v_k} \end{bmatrix}.$$

Equation 4

*Proposition 3:* Given the input (to interface from the simulation) and output (to hardware from the interface) time-series data, as in Equation 4 for a SISO interface in a HiL simulation. Then the transfer function $G_{VH}(s)$ for the interface is obtained applying the subspace identification methods.

*Proof:* Given input $(Y_v\ )$ and output $(\widehat{Y_v}\ )$ time-series measurements corresponding to the interface. Considering, $U = Y_v^d, Y = \widehat{Y_v^d}$, and applying the subspace algorithm presented in subsection 2.2 by appropriately choosing $i$, we obtain a linear discrete-time dynamical system with the system matrices, $A_d, B_d, C_d, D_d$. A continuous-time dynamical system corresponding to the discrete-time dynamical system Equation 1 is now obtained either by using zero order hold method or Tustin approximation [15]. Finally, the transfer function for the interface which is defined as the ratio of the Laplace transform of the output to the input is given by

$$G_{VH}(s) = \frac{\hat{Y}_v(s)}{Y_v(s)} = C(sI - A)^{-1}B + D,$$

where $\hat{Y}_s(s)$ and $Y_s(s)$ denote the transfer function of output and input to the interface, $A, B, C, D$ are the system matrices corresponding to the continuous-time dynamical system and $I$ is the identity matrix of appropriate size.

As with every other data-driven approach, the stability of the system learnt applying SIM depends on the nature of the data itself. This will be discussed in detail later in Section 4.0.

For multi input multi output (MIMO) system, suppose there are $q$ inputs and $q$ outputs to the interface, then we obtain a MIMO transfer function representing the interface such that, we have,

$$G_{VH}(s) = \begin{bmatrix} G_{VH}^{11}(s) & G_{VH}^{12}(s) & \cdots & G_{VH}^{1q}(s) \\ \vdots & \vdots & \ddots & \vdots \\ G_{VH}^{q1}(s) & G_{VH}^{q2}(s) & \cdots & G_{VH}^{qq}(s) \end{bmatrix}$$

<div align="center">Equation 5</div>

where $G_{VH}^{ij}(s)$ denotes the transfer function with respect to $j^{th}$ input and $i^{th}$ output. Each of these transfer functions are learnt applying Proposition 3.

From Proposition 3, we observe that the transfer function, $G_{VH}(s)$ is proper since the feed through matrix, $D \neq 0$. Therefore, the output and input Laplace transforms has the same order and can be expressed as

$$G_{VH}(s) = \frac{\hat{Y}_v(s)}{Y_v(s)} = \frac{a_n s^n + a_{n-1} s^{n-1} + \cdots + a_1 s + a_0}{b_n s^n + b_{n-1} s^{n-1} + \cdots + b_1 s + b_0}$$
$$= \frac{\sum_{i=0}^{n} b_i s^i}{\sum_{i=0}^{n} a_i s^i}$$

<div align="center">Equation 6</div>

where $n$ is the order of the transfer function and the coefficient vectors are defined as

$$b = \begin{bmatrix} b_n & b_{n-1} & \cdots & b_1 & b_0 \end{bmatrix},$$
$$a = \begin{bmatrix} a_n & a_{n-1} & \cdots & a_1 & a_0 \end{bmatrix}.$$

With the construction of transfer function of the interface, we next present a metric to quantify the transparency and there by the fidelity of the interface in the HiL simulation. From the definition of transfer function, we have,

$$\hat{Y}_v(s) = G_{VH}(s) Y_v(s)$$

<div align="center">Equation 7</div>

If the time-series data received by the hardware is as it is sent by the simulator, then it means,

$$G_{VH}(s) = 1$$

which essentially indicates that the coefficients of the numerator and the denominator are the same. This inspires the definition of transparency defined as a function of the distance metric based on the coefficients of the numerator and denominator polynomials in `s' of the transfer function as follows.

*Definition 4:* The distance between the numerator and denominator polynomials of the transfer function, $G_{VH}(s) = \frac{\widehat{Y_v}(s)}{Y_v(s)}$ is given by

$$\mathcal{D}_p = ((a_0 - b_0)^p + (a_1 - b_1)^p + \cdots + (a_n - b_n)^p)^{\frac{1}{p}}$$

<div align="center">Equation 8</div>

where $p \in \{1, 2, \dots, \infty\}$.

A similar distance metric with $p = 2$ is defined in the work [10]. The ability to compute the distance metric (that helps in studying transparency, and subsequently fidelity) for any given frequency ($s = j\omega$) motivated the transfer function based approach as opposed to the state space approach.

The distance metric defined in Equation 8 for a MIMO system results in a matrix as given by

$$\mathcal{D}_p := \begin{bmatrix} \mathcal{D}_p^{11} & \mathcal{D}_p^{12} & \cdots & \mathcal{D}_p^{1q} \\ \vdots & \vdots & \ddots & \vdots \\ \mathcal{D}_p^{q1} & \mathcal{D}_p^{q2} & \cdots & \mathcal{D}_p^{qq} \end{bmatrix}$$

<div align="center">Equation 9</div>

where $D_p^{ij}$ denote the distance metric corresponding to the transfer function $G_{VH}^{ij}(s)$ with $j^{th}$ input and $i^{th}$ output. The distance corresponding to each SISO subsystem is computed using Equation 8.

We now formally define the transparency of the HiL simulation as follows:

*Definition 5:* The transparency of the HiL simulation is defined as

$$\mathcal{T}(G_{VH}(s)) := \begin{cases} \mathcal{D}_p & \text{for SISO system} \\ \text{trace}(\mathcal{D}_p) & \text{for MIMO system} \end{cases}$$

<div align="center">Equation 10</div>

Note that by definition, the transparency of the HiL simulation is always a scalar value. For a completely transparent system, we must have $G_{VH}(s) = 1$ for SISO system and $G_{VH}(s) = I$ for MIMO system which results in $T(G_{VH}(s)) = 0$. Hence, $T \in [0, \infty)$. The greater the value of $T$, the less transparent the interface is.

Finally, we formally define the fidelity of the HiL simulation as a function of transparency as follows.

*Definition 6:* The fidelity of the HiL simulation is defined as:

$$F := \frac{1}{1 + T}$$

<span style="color:orange">Equation 11</span>

Observe that by definition, the fidelity value always lie between $(0,1]$, where the value of 1 denotes complete fidelity.

In the following section, the fidelity quantification from time-series data is illustrated on an HiL simulation.

# 4.0 Simulation Study

The data used for demonstration purposes was generated via controller hardware in the loop (CHiL) experimentation on the IEEE 123 node feeder model (see Fig. \ref{fig:123bus}). This feeder is modified to include 3 diesel generators, 3 grid-forming inverters and 3 grid-following inverters to support the loads in the feeder during islanded operation. A combination of physical and virtual (directly on the simulator) protection relays were configured for the experiment and were communicating with an open platform communication (OPC) server that serve as a data aggregator over a local area network within the testbed. In addition to the ground truth data collected directly from the simulator (OPREC format), network traffic was also captured in the form of a packet capture by setting up port mirroring on the network infrastructure.
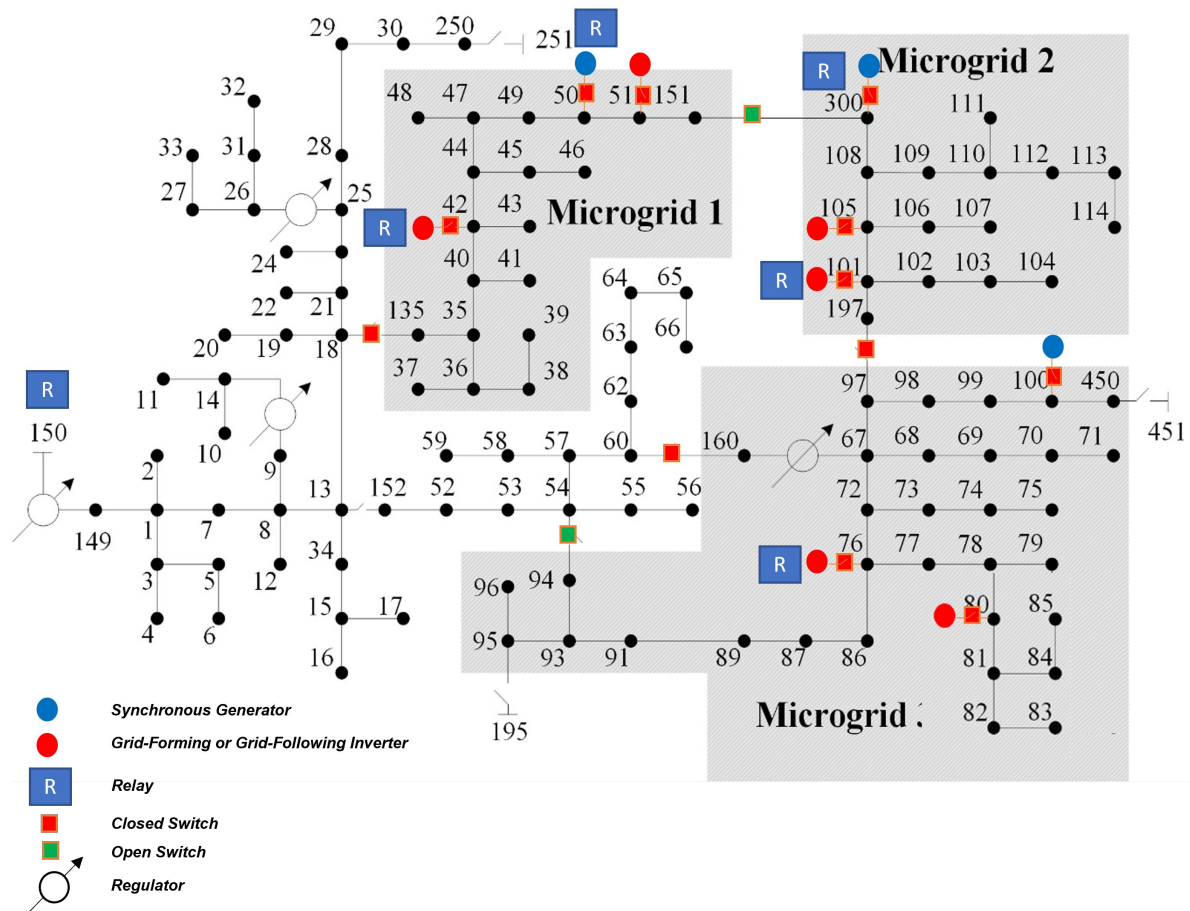


Figure 2: IEEE 123 bus feeder model with GFMs, GFLs, diesel generators , and relays.

## 4.1 Data Generation

The experimental datasets generated from the CHiL experimentation illustrate a variety of scenarios including voltage and power oscillations, load shedding, and islanded operation. The experimental platform provides multiple dataset types to monitor a variety of measurements. Network traffic packet captures (PCAP) contains all microgrid network traffic including RMS measurements, Modbus devices for inverters, physical relays, remote terminal units (RTUs), and OPC server. Proprietary OPREC data includes simulated HYPERSIM data provided to the physical devices. The microgrid test feeder model and the HiL elements were specific

instantiations on the powerNET testbed, which is a high-fidelity, flexible, multi-user cyber-physical environment [16], [17].

Each virtual remote terminal unit (VRTU) records several measurements corresponding to the network including bus RMS voltage and current, and inverter data. The data for each device is recorded over three phases. Moreover, the recorded measurements can be configured. Four virtual DNP3 devices within the HYPERSIM simulator record network traffic multiple points to provide coverage over the testbed.

Leveraging these two datasets, the team models the interface between simulation (HYPERSIM) and hardware (VRTUs) within the platform. OPREC datasets provide simulated measurements while the corresponding responses from hardware devices are provided by the PCAP datasets. In the scope of this effort, we apply the developed fidelity quantification framework to study the fidelity of the CHiL interface. However, in doing so, the first step is to process both these datasets for the fidelity computation.

## 4.2 Fidelity Study

The OPREC and PCAP measurements from the experiment on a load change scenario are considered for the Fidelity study. This data set is generated by creating two load changes. The first load change is an increase of the load to $150\%$ at around $450s$ and the second one is reduction of the load to $75\%$ at around $750s$. The OPREC measurements are available at a high time resolution of 2000 measurements every second. On the other side, the PCAP measurements recorded near the virtual RTU are available at 1 measurement every second. The PCAP measurements are interpolated to bring these two measurements to the same sampling rate and are shown in Figure 3 corresponding to two randomly chosen buses $100$ and $42$.

One of the immediate observations from Figure 3 is that the OPREC and PCAP measurements are nearly aligned for bus $100$ and for bus $42$, the PCAP measurements are received with a delay. One of the objectives of this work is to quantify the fidelity of the interface when the time-series data is communicated via the interface. In other words, if there are any delays, signal attenuation or amplification, or noise corruption happening as a result of passing through the interface, it will reflect in as a lowered fidelity measure.

As there are several measurements recorded by each virtual RTU, for the fidelity study, the interface connecting each VRTU and the HYPERSIM simulator is studied independently. Furthermore, fidelity with respect to every (three-phase) measurement between all the VRTU and the HYPERSIM simulator is also studied.
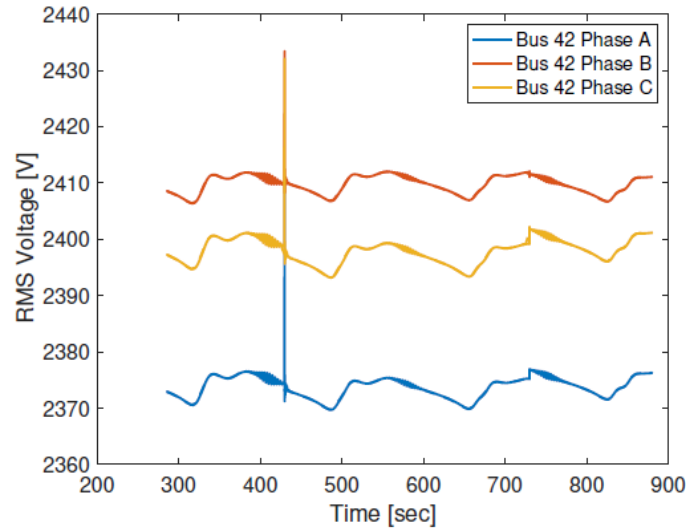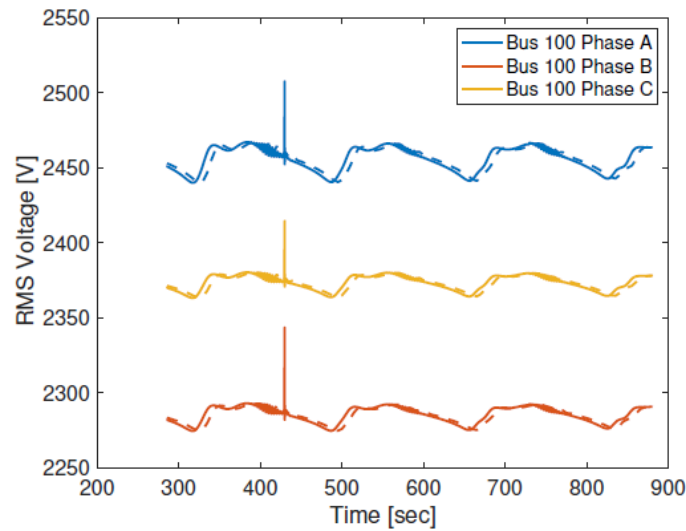
Figure 3: (a) RMS Voltage at bus 100 and (b) RMS Voltage at bus 42 during the course of the HiL simulation. The solid lines indicate the OPREC measurements, and the dotted lines indicate the PCAP measurements.

The OPREC measurements from the simulator are considered as input measurements ($U$) and the PCAP measurements recorded by the VRTUs is considered as the output measurements ($Y$). Using these input and output measurements, a linear system is obtained governing this data by applying the subspace identification algorithm discussed in Algorithm 1. The corresponding Fidelity values when the Inverter 42 set-points are modified are shown in Figure 4 (a) and (b) respectively. For this analysis, the value of $i$ is chosen to be $4$ (see Equation 2, and the subsequent discussion for more details), $p = 2$ (see Equation 8) and the learnt linear system is chosen to be of order $1$. For the chosen values of $i, p$ and the order of the system, the resultant (learnt) system is stable.
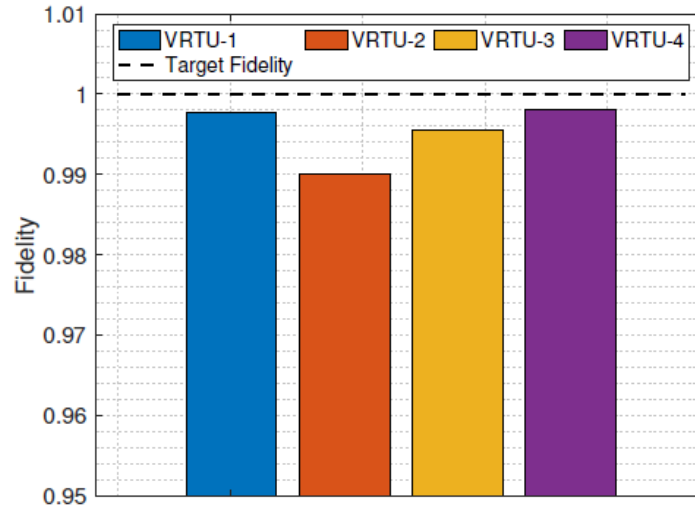
(a)
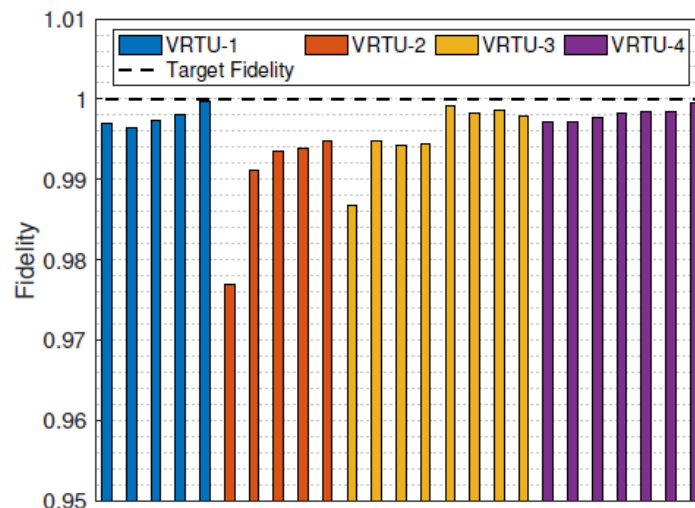


(b)

Figure 4: Fidelity of the interface when Inv 42 set-points are changed. (a) Fidelity when each VRTU is studied independently (b) Fidelity with respect to each three-phase measurement.

From Figure 4, it is observed that the interface with VRTU-1 has a high fidelity since it is close to 1 and the interface with VRTU-2 is seen to be having relatively low fidelity. This relatively lower fidelity is attributed to the delay in the measurements similar to that seen in Figure 3 (b) which reflected on the learnt transfer function for the VRTU-2 interface. Note that to account for delays, usually additional exponential terms are accounted for yielding an irrational transfer function. However, as the objective here is not to quantify the delay but instead to understand the fidelity, we restricted to finding a rational transfer function.

To better understand how the fidelity is affected for a different operating state of the HiL simulation, another scenario where the load changes were modified is considered. Figure 5

shows the Fidelity of each of the VRTU interfaces. Although the relatively highest and lowest fidelity when compared to the Inv 42 study remains unchanged, the relative rank ordering of each of the VRTU interfaces in Inv 42 study and this load change study are different. This show the effect of the operating state of the HiL simulation on the Fidelity characterization.
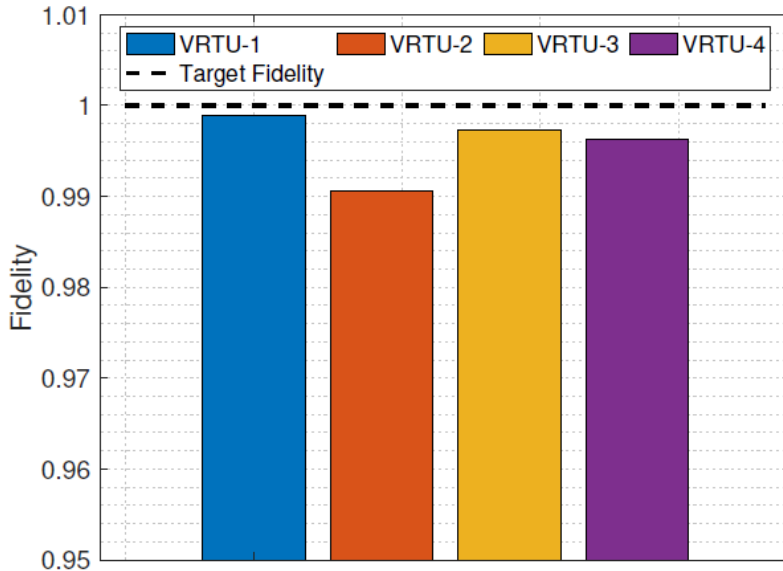


Figure 5: Fidelity of each of the VRTU interface during load changes in the HiL simulation of the IEEE 123 node feeder model.

The proposed fidelity quantification framework is furthermore not sensitive to the choice of the order of the system. To corroborate this, the linear system is learnt with different orders as shown in Figure 6. The values, $i = 4$ (see the discussion after Equation 2), $p = 2$ (see Equation 8) are chosen for all the cases and the learnt linear systems are stable. Vacuously, different choice of the system order has not changed the interpretation of the Fidelity.
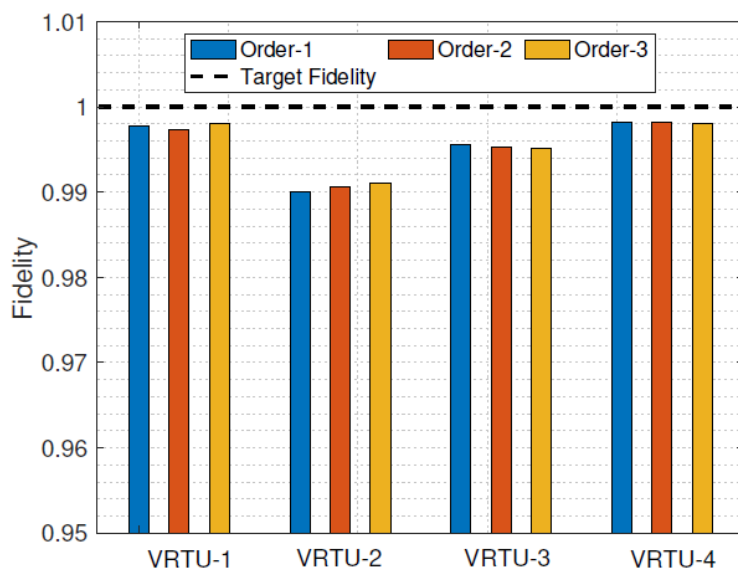


Figure 6: Fidelity corresponding to the INV 42 study with various choices of system order.

# 5.0 Conclusion

In this work, we developed a systematic framework to analyze the fidelity of the interface in a HiL simulation. In particular, we presented a data-driven framework to determine the fidelity using the subspace identification method (SIM). The proposed fidelity characterization involves learning a linear system for the interface between the simulator and the hardware using the SIM and studying its transfer function. This approach is valid for SISO as well as MIMO HiL systems and is applied to understand the fidelity of the IEEE 123 node feeder model in HYPERSIM simulator interacting with virtual RTUs. From this study, it is seen that Fidelity not only depends on the type of interface but also a function of the operating state. Future work involves developing fidelity characterization between two different simulators.

# 6.0 References

[1] D. C. Gross et al., "Report from the fidelity implementation study group," in Fall Simulation Interoperability Workshop Papers, 1999.

[2] M. Roza, J. Voogd, H. Jense, and P. Van Gool, "Fidelity requirements specification: A process oriented view," in Fall Simulation Interoperability Workshop. Citeseer, 1999.

[3] Department of Defense, "Modeling and simulation (m&s) glossary," https://www.acqnotes.com/Attachments/DoD%20M&S%20Glossary%201%20Oct%2011.pdf, accessed: 2022-10-10.

[4] Z. Roza, D. Gross, and S. Harmon, "Report out of the fidelity experimentation isg," complexity, vol. 4, no. 11, p. 12, 2000.

[5] A. H. Feinstein and H. M. Cannon, "Fidelity, verifiability, and validity of simulation: Constructs for evaluation," in Developments in Business Simulation and Experiential Learning: Proceedings of the Annual ABSEL conference, vol. 28, 2001.

[6] Z. C. Roza, "Simulation fidelity theory and practice: A unified approach to defining, specifying and measuring the realism of simulations. "Ph.D. dissertation, Delft University of Technology, 2004.

[7] W. Ren, "Accuracy evaluation of power hardware-in-the-loop simulation, "Ph. D. dissertation, ECE Dept, 2007.

[8] M. MacDiarmid and M. Bacic, "Quantifying the accuracy of hardware in-the-loop simulations," in 2007 American Control Conference. IEEE, 2007, pp. 5147–5152.

[9] Typhoon HIL, Inc, "Ultra-high fidelity controller hardware-in-the-loop (chil) nanosecond resolution "flight simulator" for future grid," https://www.nrel.gov/grid/assets/pdfs/gridsim-d117-celanovictyphoonhil.pdf, accessed: 2022-10-10.

[10] C. Koehler, A. Mayer, and A. Herkersdorf, "Determining the fidelity of hardware-in-the-loop simulation coupling systems," in 2008 IEEE International Behavioral Modeling and Simulation Workshop. IEEE,2008, pp. 13–18.

[11] G. F. Lauss, M. O. Faruque, K. Schoder, C. Dufour, A. Viehweider, and J. Langston, "Characteristics and design of power hardware-in-the-loop simulations for electrical power systems," IEEE Transactions on Industrial Electronics, vol. 63, no. 1, pp. 406–417, 2015.

[12] S. saagar Ponnusamy et al., "Simulation product fidelity: a qualitative& quantitative system engineering approach," Ph.D. dissertation, Toulouse 3, 2016.

[13] P. Van Overschee and B. De Moor, Subspace identification for linear systems: Theory—Implementation—Applications. Springer Science &Business Media, 2012.

[14] H. J. Palanthandalam-Madapusi, S. Lacy, J. B. Hoagg, and D. S.Bernstein, "Subspace-based identification for linear and nonlinear systems," in Proceedings of the 2005, American Control Conference,2005. IEEE, 2005, pp. 2320–2334.

[15] G. F. Franklin, J. D. Powell, M. L. Workman et al., Digital control of dynamic systems. Addison-wesley Reading, MA, 1998, vol. 3.

[16] T. Edgar, D. Manz, and T. Carroll, "Towards an experimental testbed facility for cyber-physical security research," in Proceedings of the Seventh Annual Workshop on Cyber Security and Information Intelligence Research, 2011, pp. 1–1.

[17] A. Ashok, S. Sridhar, T. Becejac, T. Rice, M. Engels, S. Harpool,M. Rice, and T. Edgar, "A multi-level fidelity microgrid testbed model for cybersecurity experimentation," in 12th USENIX Workshop on Cyber Security Experimentation and Test (CSET 19), 2019.

**Pacific Northwest
National Laboratory**

902 Battelle Boulevard
P.O. Box 999
Richland, WA 99354

1-888-375-PNNL (7665)

*www.pnnl.gov*